Indentation deformation mechanism in glass: Densification versus shear flow

T. Rouxel,[1,a)] H. Ji,[1] J. P. Guin,[1] F. Augereau,[2] and B. Rufflé[3]
[1]*Applied Mechanics Laboratory of the University of Rennes 1, LARMAUR, ERL CNRS 6274, Université de Rennes 1, Campus de Beaulieu, 35042 Rennes cedex, France*
[2]*LAIN, UMR 5011, CNRS-Université Montpellier II, Place E. Bataillon, CC 082, F-3409 Montpellier cedex, France*
[3]*LCVN, UMR 5587, CNRS-Université Montpellier II, Place E. Bataillon, CC 082, F-3409 Montpellier cedex, France*

(Received 15 January 2010; accepted 26 March 2010; published online 7 May 2010)

Although the characteristic time constant for viscous relaxation of glass is so large at room temperature that viscous flow would be hardly detectable, a permanent deformation can be easily achieved at ambient temperature by applying a sharp contact loading—a Vickers indenter for instance—for few seconds only. We provide direct evidence for densification and volume conservative shear flow by means of atomic force microscopy topological analysis of the indentation profile and volume on as-quenched and densified specimens (pressure up to 25 GPa). We show that both possible mechanisms contribute to different extents depending on the glass composition. A major finding is that densification predominates in glasses with relatively low atomic packing density but that shear flow relays on once densification is achieved. © *2010 American Institute of Physics*. [doi:10.1063/1.3407559]

I. INTRODUCTION

Glasses are brittle materials and fail in a purely elastic manner at room temperature. Nevertheless it is possible to induce a permanent deformation using a sharp indenter. This is the way hardness—a measure of the mean contact stress for the formation of a permanent imprint—is estimated. Typical values for glass hardness range between 1 (chalcogenides) and 7 (silica-rich) GPa. These values are obviously much larger than those applied during classical mechanical testing or in service conditions and are sufficient to generate some densification in a process zone beneath the indentation. There as been a long lasting controversy about the nature of the permanent indentation deformation. Although a classical plasticity approach was first considered,[1] the indentation deformation proved later to be nonvolume conservative[2,3] and to exhibit a time dependence (indentation-creep) at room temperature. This calls for caution regarding the definition of plastic yield stress and the use of standard equations for elastoplasticity in the case of glasses. Densification beneath the indentation was deduced from changes in the refractive index as measured by optical interferometry and was recognized to be a general property of glasses.[2,3] Nevertheless, there are observations of shear lines and pileup suggesting the occurrence of shear flow at room temperature.[3–6] Densification involves a collapse of matter into a more close-packed structure and is a displacive transformation. The smaller the atomic packing density is, the larger the magnitude of the volume shrinkage.[7] In the case of amorphous silica (a-SiO_2), densification accounts for 80% of the indentation volume, whereas for a Zr-based metallic glass, it contributes to less than 10% of the deformation.[8] On the contrary, shear flow is reconstructive. As a matter of fact shear flow results in the piling-up of matter in the vicinity of the indentation whereas densification leaves a well defined indent surrounded by a weakly distorted flat surface. Note that both mechanisms are thermally activated but the activation energy associated to the densification process was found much smaller than the one for shear flow [511 and 35–55 kJ mol^{-1}, respectively, for a-SiO_2 (Refs. 9 and 10)] and unlike densification, shear flow is not kinematically bounded. Consequently the contribution of shear flows is expected to increase rapidly with the loading time and with temperature or, for glasses with different T_g values, will tend to decrease with rising T_g at a given temperature.[11]

II. MATERIALS AND EXPERIMENTAL PROCEDURES

In this work, we show that there is a strong effect of the glass composition on the relative importance of each contribution and that a direct estimation is possible by means of a detailed topological analysis of the indentation site using atomic force microscopy (AFM). We compare the indentation behavior of as-quenched (pristine) and pressure-densified glasses from different chemical systems including a soda-lime-silica window glass (WG) and a $Zr_{55}Cu_{30}Ni_{10}Al_5$ bulk metallic glass (BMG), covering a wide range of T_g values (numbers in brackets, in kelvin): a-SiO_2 (1463), WG (835), $GeSe_4$ (435), and BMG (673). Some pure platinum [99.99% pure, Superpure Chemetals, NJ (USA)] was also investigated as a model material with high packing density behaving in an elastoplastic manner with no volume change upon plastic deformation. Pressure-densified specimens were obtained by means of an octahedral multianvil apparatus using a Walker cell and following a procedure described elsewhere.[7,12] Each run consisted in raising the load pressure of the main ram at a rate of 0.5 MPa per minute. After reach-

a)Electronic mail: tanguy.rouxel@univ-rennes1.fr.

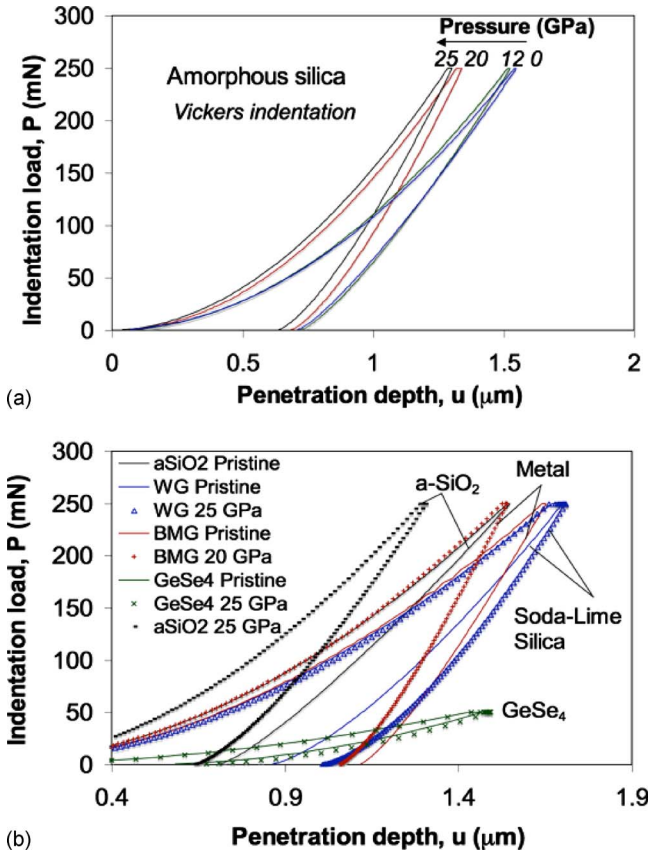

FIG. 1. (Color online) Load-depth data for loading-unloading cycles using a Vickers indenter on (a) a-SiO_2 glass specimens after high pressure treatments, and (b) various glasses before and after high pressure treatments.

ing the pressure target, the specimens were maintained at high pressure for 1 h and then slowly unloaded. It is noteworthy that unlike previously reported high pressure investigation specimens did not fracture during the experiments, suggesting that the pressure device induced very little shear. These glasses were indented using a Vickers indenter (pyramidal diamond with 148.1° edge to edge apical angle) under a 50 (for $GeSe_4$), 100 (for a-SiO_2 and WG), and 250 mN (for BMG) load for 15 s. This load was chosen low enough to prevent against visible surface radial microcracking. Then the indentation profiles and volumes were estimated from AFM measurements using a dedicated routine described elsewhere.[8] The elastic moduli of the densified specimens were characterized by means of Brillouin scattering spectroscopy[13] and acoustic microscopy following experimental procedures described in Ref. 14 The combined use of these two techniques provides accurate values for the sound wave velocities V_L and V_T.

III. HIGH PRESSURE TREATMENT EFFECTS ON THE ELASTIC PROPERTIES

The comparison between the loading (up to 250 mN) unloading curves obtained on pristine and high pressure specimens (Fig. 1) shows significant differences in the case of pressure sensitive glasses. For instance, the penetration depth decreases from 1.53 μm for the pristine a-SiO_2 glass to 1.29 μm for the glass densified under 25 GPa. Correlatively, Young's modulus increases with the densification process and hardness follows the same trend in all cases but for WG (Table I). In this latter case, for pressure above 8 GPa, a slight decrease in hardness is observed (by 7% for pressure over 20 GPa). The abrupt increase in the pile-up volume for pressure above 8 GPa indicates that the contribution of shear

TABLE I. Predensification and postdensification physical and mechanical properties of the glasses (nm: not-measured).

Glass	Pressure (GPa)[a]	ρ (kg m^{-3}) [b]	E (GPa)	ν [d]	Hv (GPa)	V^+/V^- [e] (%)
a-SiO_2	0	2.199	74.5	0.150	8.35	17
a-SiO_2	12	2.262	75.9	0.149	8.12	nm
a-SiO_2	20	2.654	104.5	0.212	10.80	nm
a-SiO_2	25	2.674	109	0.252	11.48	77
WG	0	2.514	71.5	0.230	6.25	22
WG	8	2.517	74.8[c]	nm	6.34	nm
WG	20	2.672	78.4	0.228	5.82	38
WG	25	2.672	77.8[c]	nm	5.75	38
$GeSe_4$	0	4.337	14.8	0.286	1.39	61
$GeSe_4$	3	4.396	15.5[c]	nm	1.44	nm
$GeSe_4$	25	4.402	17.1[c]	nm	1.47	63
BMG	0	6.830	81.6	0.380	5.53	34
BMG	10	6.864	105.4[c]	nm	5.60	nm
BMG	20	6.932	104.4[c]	nm	5.65	35
Platinum	0	21.45	168	0.380	0.59	75

[a]Hydrostatic pressure applied for 1 h.
[b]Density measured with a better than 0.001 g cm^{-3} accuracy by means of a density gradient method using partially miscible heavy liquors (Ref. 7).
[c]Reduced Young's modulus as determined by instrumented indentation method: $E^*=E/(1-\nu^2)$.
[d]Poisson's ratio as calculated from the acoustic wave velocities $\{\nu=(V_l^2-2V_t^2)/[2(V_l^2-V_t^2)]\}$.
[e]V^+ and V^- are the volumes of piled-up material around the indent and of the indentation print, respectively, as measured by AFM.

flow to the indentation deformation strongly increased, as will be discussed below. The increase is particularly significant in the case of a-SiO_2: 46% and 37% increase in Young's modulus (E) and Vickers hardness (Hv), respectively. In cases where E was not directly measured, the reduced Young's modulus [$E^*=E/(1-\nu^2)$ where ν is Poisson's ratio] was derived from the unloading portion of the instrumented indentation curves. The E^* values confirm the tendency, even for glasses with larger atomic packing densities such as chalcogenide and BMGs which experience minor changes under high pressure testing. Nevertheless slight differences are observed between E^* and E. This is likely because the studied glasses have significantly varying Poisson's ratio and elastic moduli and hence lead to different indentation deformation mechanisms and indentation profiles, as discussed further. Poisson's ratio is found to increase with pressure, in agreement with previous investigations on a-SiO_2.[15] This reflects an increase in the atomic packing density as well as a decrease in the short to medium-range ordering (larger intertetrahedral angle distribution, tendency to larger coordination number for Si).

IV. THE PERMANENT DEFORMATION MECHANISMS OF GLASS IN AMBIENT CONDITIONS

The physics of permanent deformation of glass at ambient temperature under sharp contact loading has long been intriguing especially since glasses are regarded as model brittle linear elastic materials. On one hand classical plasticity based on dislocation mobility is not expected since glasses lack long range structural ordering at the atomic scale. On the other hand viscous flow at ambient temperature would require incredibly long times to be detected on the basis of the newtonian shear viscosity coefficient.[16] Nevertheless densification has been evidenced and there are convincing studies of shear-thinning indentation flow.[17,18] Direct evidence for both mechanisms and for the predominance of densification below T_g was recently reported in synthetic clay which showed up as a good glass "analogue" material to study the permanent deformation mechanisms.[19]

The primary response of the glass to the sharp contact loading is an almost instantaneous elastic sinking of the surface. Assuming pure linear elasticity, the equilibrium mean contact pressure (elastic hardness) for a rigid conical indenter of apical angle 2ϕ is expressed as:[20]

$$H_{el} = E/[2(1-\nu^2)\tan\phi]. \quad (1)$$

As a first approximation a Vickers indenter can be assimilated to a cone indenter producing the same projected surface area. This gives $\phi=70.3°$ for this equivalent cone indenter. It follows that H_{el}=13.6, 13.5, 2.89, and 17.1 GPa for a-SiO_2, WG, $GeSe_4$, and BMG glass, respectively. These values are typically 2 to 3 times larger than hardness values and are large enough to promote densification in pressure sensitive glasses. Thus, in a secondary stage, irreversible microscopic deformation events aiming at efficiently relaxing the contact stress by increasing the contact surface area will initiate in a process zone near the indenter tip (Fig. 2). The deformation mechanism is either densification in glasses with relatively low atomic packing density, or volume conservative shear flow in glasses with close-packed atomic network, or a combination of both in general.

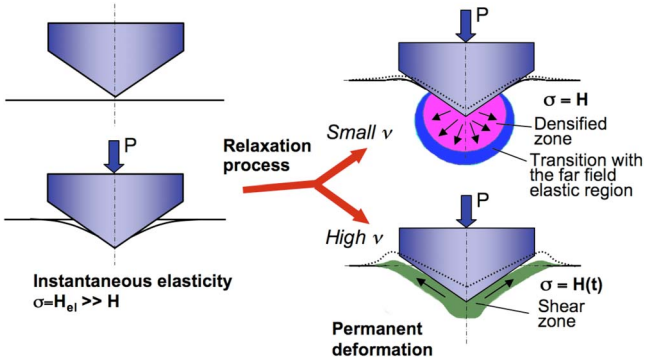

FIG. 2. (Color online) Schematic sketch of the indentation deformation stages. The dashed line indicates the indentation profile after unloading. Arrows indicate matter displacement. σ is the mean contact pressure.

In the case of densification, the depth of the affected zone beneath the indenter (z_d) can be roughly estimated by using the Boussinesq's elastic stress field[21] stemming from a contact force (F), assuming densification becomes negligible once the hydrostatic stress is smaller than the pressure P_o corresponding to the onset of the densification process (from high pressure experiments), and saturates rapidly above P_o (Refs. 7 and 22)

$$z_d = [F(1+\nu)/(3\pi P_o)]^{1/2}. \quad (2)$$

With a contact force of 3.9 N and in the case of a-SiO_2 [taking ν=0.15 (pristine) to 0.252 (densified), P_o=8 GPa (Ref. 7)], then z_d=7.7–8.1 μm which is in excellent agreement with the value (8 μm) of the depth of the zone where a change of the refractive index was observed for the same load in a-SiO_2.[2] Raman scattering was recently used to map the densification in a vertical cross section through a 19.6 N Vickers indent in a-SiO_2.[23] Isodensification domains were drawn. Again the depth experimentally found for the densified zone (18 μm) is corroborated by the value for z_d (17.3 μm). Besides assuming a paraboloid shape for the isodensification domains, integration of the volume shrinkage through the overall densified area leads to a contribution of densification to the indentation volume of ~85%, in good agreement with previous investigations at lower loads (90% in Ref. 8). Interestingly once a-SiO_2 is densified ν increases (from 0.15 to 0.25) and piling-up is observed (Figs. 3 and 4). The dramatic increase in V^+/V^- ratio from 17% to 77% shows that shear flow accounts for most of the deformation and to a greater extent than in the case of $GeSe_4$ and BMG, although there is almost no room for the densification contribution in BMG.[7,8] Our topological characterization (Table I, Fig. 4) also shows that shear flow is more important in densified silica than in densified WG. In this latter case V^+/V^- is limited to 38% and a decrease in hardness is observed after treatments under pressure over 20 GPa. A tentative explanation is that in such glass where both densification and shear have significant contributions, the structural changes induced by the high presure treatments (decrease in the mean intertetrahedral angle for instance[5,7]) and the cor-

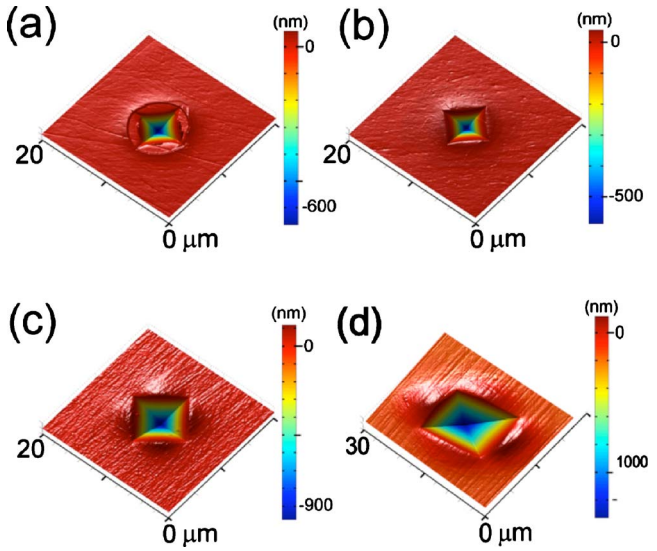

FIG. 3. (Color online) AFM observations of Vickers indents performed uner 100 mN at the surface of (a) a-SiO_2 pristine glass; (b) a-SiO_2 after 1 h under 25 GPa hydrostatic pressure; (c) BMG pristine glass; and (d) pure Platinum in the same experimental conditions (reported for comparison). Note the disappearance of the Hertzian cone crack and the raise of a pile-up of matter after pressure treatment.

responding increase in Poisson's ratio favor shear to such an extent that the glass appears slightly softer than before densification. In a previous study, it was found that for pristine silica glass, the refractive index of the glass immediately surrounding the indentation is different from that of the bulk.[24] Therefore, it is suggested that once densification is achieved, shear flows relays on and the densified zone is partially squeezed-out toward the surface where it piles-up. Nevertheless, in cases where volume conservative flow is the dominant mechanism the pile-up volume remains noticeably smaller than the indentation volume: $V^+/V^-=34\%$, 61%, and 75% for BMG $GeSe_4$, and pure platinum, respectively. The case of pure platinum (polycrystalline), which is discussed

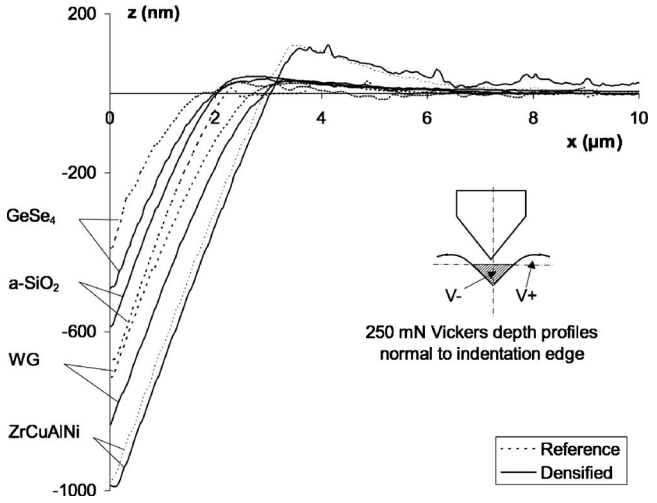

FIG. 4. AFM characterization of the indentation profiles (only half of the profile is displayed) through the center of the Vickers indent, normal to the edge (pile-up is less pronounced in a cross-sections containing the indent diagonals). Inset shows the V^+ and V^- volumes estimated from AFM scanning of the indents.

here for comparison, demonstrates that even for a dense material behaving purely plastic $V^+ < V^-$. This is because a significant fraction of material has been moved downwards in the bulk where it is responsible for postunloading residual stresses. The residual elastic stress field prevents against a complete recovery of the elastic energy stored during the loading stage and is responsible for the radial-median cracks observed at higher loads in brittle solids. It is noteworthy that the V^+/V^- values are in good agreement with those reported for synthetic clay below T_g ($V^+/V^-=13\%$), i.e., in a range where the material contains a significant fraction of porosity, and above T_g ($V^+/V^-=65\%$) where deformation mainly proceeds by means of a volume conservative shear process.[19] Although indentation volume measurements were not carried out for all specimens, the fact that a relatively well defined pressure threshold exists for the onset of the densification process, located at around 3 GPa for $GeSe_4$ and 10 GPa for both WG and a-SiO_2, with a saturation at 20 GPa for the two latter glasses,[7] suggests very similar results for $GeSe_4$ at 3 GPa, for WG at 8 GPa, and for a-SiO_2 at 12 and 20 GPa, than for the same glasses at 0 GPa, 0 GPa, 0 GPa, and 25 GPa, respectively.

Regarding the shear flow mechanism it was reported that this process is relatively more thermally activated than densification (approximately one order of magnitude difference for the activation energies[9,10]) so that shear flow takes over densification at temperature from near—and above—T_g but is much reduced and perhaps nonexistent at low temperature.[6,19] Having relatively low T_g temperatures, chalcogenide and to a lesser extent BMGs are potential candidates for this mechanism. Extrapolation of the viscosity curves to 293 K would give values between 10^{20} and 10^{30} Pa s. With these values and assuming a linear elastoviscous behavior with a Newtonian viscous flow, durations of the order of thousand years would be predicted to reach the actual hardness values measured at ambient temperature after 15 s loading time. The time-dependence of hardness writes

$$H(t) = \mu/[(1-\nu)(1+t/\tau)\tan\phi], \quad (3)$$

where $\tau = \eta/\mu$ is the characteristic relaxation time and μ is the shear modulus.[11,25] Note that this expression reduces to Eq. (1) for purely elastic materials ($\eta \to \infty$). However, both viscosity measurements and numerical simulation provide evidence for a sharp viscosity drop at high stress or strain-rate levels.[10,26,27] This is called shear-thinning and is favored in weakly polymerized network structures. Although a description of the indentation problem in the light of nonlinear flow is far beyond the scope of this paper, it is anticipated that for shear stresses in the gigapascal order viscosity may drop of orders of magnitude. The piling-up of matter is representative of the volume conservative shear flow process. It has been extensively reported for crystals.[28] The contribution of shear flow becomes larger than 20% of the indentation print in glasses with Poisson's ratio over 0.25 (60% for $GeSe_4$). Note that in $GeSe_4$ the indentation testing duration is too small to allow for viscous flow so that most of the elastic energy stored upon loading is released during unloading. The differences observed between glasses with different Poisson's ratio are also observed in a given chemical system by

varying the composition. For instance, in chalcogenide glasses an increase in the mean coordination number (up to 2.4 corresponding to the percolation threshold), which is associated with a decrease in ν, results in a decrease in the pile-up height.[29] The incidence of Poisson's ratio stems from the fact that although ν is defined for small strain elastic perturbations only it is correlated with the packing density (open structures exhibit low ν values and can be densified, whereas materials with $\nu=1/2$ are incompressible and solely deform by means of shear processes).[30]

V. CONCLUSION

In conclusion, this study of the indentation deformation process in glass shows that densification predominates over shear flow in glasses with relatively low atomic packing density. However, after very high pressure cycles (over 10 GPa), deformation chiefly proceeds by means of volume conservative shear flow, even in the case of a-SiO_2. Besides, Poisson's ratio (ν) shows up as a remarkable index to discriminate between both mechanisms. A major finding is that the shear flow contribution is higher in densified a-SiO_2 than in densified WG although it is very limited and perhaps nonexistent in the pristine glass. In contrast to crystalline materials and especially metals, for which hardness number is a measure of the shear stress required to initiate plastic flow, hardness of a glass as determined with a sharp indenter can be defined either as the resistance of a material to densification in the case of low ν, as a resistance to volume conservative shear flow (high ν glasses), or as the combination of both in the general case.

ACKNOWLEDGMENTS

The authors are grateful to Professor Y. Kawamura from Kumamoto University (Japan) and to the LVC team of the UMR-CNRS 6226 (Rennes, France) for providing, respectively, the BMG and the $GeSe_4$ glass specimens. Funding for this project was provided by the Ministry of Research and Higher Education (Grant No. HJ130876-1207).

[1] D. M. Marsh, Proc. R. Soc. London **282A**, 33 (1964).
[2] F. M. Ernsberger, J. Am. Ceram. Soc. **51**, 545 (1968).
[3] K. W. Peter, J. Non-Cryst. Solids **5**, 103 (1970).
[4] E. Dick, Glastech. Ber. **43**, 16 (1970).
[5] J. T. Hagan and S. Van Der Zwaag, J. Non-Cryst. Solids **64**, 249 (1984).
[6] C. R. Kurkjian, G. W. Kammlott, and M. M. Chaudhri, J. Am. Ceram. Soc. **78**, 737 (1995).
[7] T. Rouxel, H. Ji, T. Hammouda, and A. Moréac, Phys. Rev. Lett. **100**, 225501 (2008).
[8] S. Yoshida, J.-C. Sangleboeuf, and T. Rouxel, J. Mater. Res. **20**, 3404 (2005).
[9] J. D. Mackenzie, J. Am. Ceram. Soc. **46**, 461 (1963).
[10] S. Yoshida, S. Isono, J. Matsuoka, and N. Soga, J. Am. Ceram. Soc. **84**, 2141 (2001).
[11] H. Shang and T. Rouxel, J. Am. Ceram. Soc. **88**, 2625 (2005).
[12] T. Hammouda, Earth Planet. Sci. Lett. **214**, 357 (2003).
[13] R. Vacher, S. Ayrinhac, M. Foret, B. Rufflé, and E. Courtens, Phys. Rev. B **74**, 012203 (2006).
[14] R. J. M. DaFonseca, Adv. Mater. **5**, 508 (1993).
[15] C.-S. Zha, R. J. Hemley, H.-K. Mao, T. S. Duffy, and C. Meade, Phys. Rev. B **50**, 13105 (1994).
[16] E. D. Zanotto, Am. J. Phys. **66**, 392 (1998); **67**, 260 (1999).
[17] W. T. Han and M. Tomozawa, J. Am. Ceram. Soc. **73**, 3626 (1990).
[18] P. Grau, G. Berg, H. Meinhard, and S. Mosch, J. Am. Ceram. Soc. **81**, 1557 (1998).
[19] H. Ji, E. Robin, and T. Rouxel, Mech. Mater. **41**, 199 (2009).
[20] A. E. H. Love, Q. J. Math. **os-10**, 161 (1939).
[21] J. Boussinesq, *Applications des potentiels à l'étude de l'équilibre et du mouvement des solides élastiques* (Gauthier-Villars, Paris, 1885).
[22] M. Grimsditch, Phys. Rev. Lett. **52**, 2379 (1984).
[23] A. Perriot, D. Vandembroucq, E. Barthel, V. Martinez, L. Grosvalet, C. Martinet, and B. Champagnon, J. Am. Ceram. Soc. **89**, 596 (2006).
[24] W. B. Hillig, in *Advances in Glass Technology, Part 2*, edited by F. R. Matson and G. E. Rindome (Plenum, New York, 1963), p. 51.
[25] T. C. T. Ting, J. Appl. Mech. **33**, 845 (1966).
[26] D. M. Heyes, J. J. Kim, C. J. Montrose, and T. A. Litovitz, J. Chem. Phys. **73**, 3987 (1980).
[27] J. H. Simmons, R. Ochoa, K. D. Simmons, and J. J. Mills, J. Non-Cryst. Solids **105**, 313 (1988).
[28] S. Tolansky, *Surface Microtopography* (Interscience, New York, 1960), 197.
[29] A. K. Varshneya, D. J. Mauro, B. Rangarajan, and B. F. Bowden, J. Am. Ceram. Soc. **90**, 177 (2007).
[30] T. Rouxel, J. Am. Ceram. Soc. **90**, 3019 (2007).